ORIGINAL PAPER

Coronary arterial dynamics computation with medical-image-based time-dependent anatomical models and element-based zero-stress state estimates

Kenji Takizawa · Ryo Torii · Hirokazu Takagi · Tayfun E. Tezduyar · Xiao Y. Xu

Abstract We propose a method for coronary arterial dynamics computation with medical-image-based time-dependent anatomical models. The objective is to improve the computational analysis of coronary arteries for better understanding of the links between the atherosclerosis development and mechanical stimuli such as endothelial wall shear stress and structural stress in the arterial wall. The method has two components. The first one is element-based zero-stress (ZS) state estimation, which is an alternative to prestress calculation. The second one is a "mixed ZS state" approach, where the ZS states for different elements in the structural mechanics mesh are estimated with reference configurations based on medical images coming from different instants within the cardiac cycle. We demonstrate the robustness of the method in a patient-specific coronary arterial dynamics computation where the motion of a thin strip along the arterial surface and two cut surfaces at the arterial ends is specified to match the motion extracted from the medical images.

K. Takizawa · H. Takagi
Department of Modern Mechanical Engineering and Waseda Institute for Advanced Study, Waseda University, 1-6-1 Nishi-Waseda, Shinjuku-ku, Tokyo 169-8050, Japan
e-mail: Kenji.Takizawa@tafsm.org

R. Torii (✉)
Mechanical Engineering, University College London, Torrington Place, London WC1E 7JE, UK
e-mail: r.torii@ucl.ac.uk

T. E. Tezduyar
Mechanical Engineering, Rice University, MS 321, 6100 Main Street, Houston, TX 77005, USA

X. Y. Xu
Department of Chemical Engineering, Imperial College London, South Kensington Campus, London SW7 2AZ, UK

1 Introduction

Computational analysis in cardiovascular fluid and solid mechanics now has powerful methods, encouraging the development of even more powerful ones, and can deal with a wide range of biomechanics problems, encouraging efforts to further increase that range. For examples of the methods developed and problems analyzed, see [1–32]. In this paper we focus on the human coronary arteries, specifically the right coronary artery (RCA).

The coronary arteries, feeding arteries to the myocardium, are known as common sites of atherosclerotic narrowing, which typically leads to myocardial infarction and sudden cardiac death [33]. Links have been suggested between the atherosclerosis development and mechanical stimuli such as endothelial wall shear stress (WSS) and structural stress in the arterial wall [34,35]. This has motivated studies on quantification of the biomechanical stresses with computational fluid and structural mechanics methods and medical-image-based anatomical models. Among such studies, those on structural mechanics [36] and fluid–structure interaction (FSI) [37,38] are rather sparse compared to those on fluid mechanics and WSS [39,40]. One reason for that is the difficulty in acquiring the wall thickness and the motion of a coronary artery, which is substantial in the RCA. Approaches used for acquiring such time-dependent anatomical data [39,41–43] include the time-dependent anatomical-model extraction method introduced in [43], which is based fully on magnetic resonance imaging (MRI). This MRI-based method was used

Springer

in [43] for blood flow analysis with cardiac-induced arterial motion.

In this paper, we focus on coronary arterial dynamics analysis, with the medical-image-based time-dependent anatomical model coming from [43]. The long-term objective is to have a better understanding of the interaction between the blood flow and arterial dynamics, which is difficult to observe experimentally. This requires FSI analysis, which in turn requires a robust method for the coronary arterial dynamics computation. The method has to be able to deal with the computational challenges involved, such as the large deformation of an incompressible material, including stretch, bending and torsion.

Medical-image-based arterial geometries come from configurations that are not stress-free. Therefore coronary arterial dynamics computations with such time-dependent anatomical models require prestress calculations or zero-stress (ZS) state estimations. More explanation of this requirement and references to some of the methods introduced to meet this requirement can be found in [28]. The methods mentioned in [28] include the original version of the technique for calculating an estimated zero-pressure (EZP) arterial geometry [44], and newer EZP versions introduced in [10,17,45], which were also presented in [19,22]. They also include the prestress technique introduced in [15] and further refined in [18], which was also presented in [19,22].

A method was introduced in [28] for element-based ZS state estimation. The method has three parts. 1. An iterative method, which starts with an initial guess for the ZS state, is used for computing the element-based ZS state such that when a given pressure load is applied, the image-based target shape is matched. 2. A method for straight-tube geometries with single and multiple layers is used for computing the element-based ZS state so that we match the given diameter and longitudinal stretch in the target configuration and the "opening angle." 3. An element-based mapping between the arterial and straight-tube configurations is used for mapping from the arterial configuration to the straight-tube configuration, and for mapping the estimated ZS state of the straight tube back to the arterial configuration, to be used as the initial guess for the iterative method that matches the image-based target shape.

In coronary arterial dynamics computation with medical-image-based time-dependent anatomical model, the method we use for the ZS state estimation has two components. The first one is the method introduced in [28] for element-based ZS state estimation. The second one is a "mixed ZS state" approach, where the ZS states for different elements in the structural mechanics mesh are estimated with reference configurations based on medical images coming from different instants within the cardiac cycle. The overall method used in the coronary arterial dynamics computation carried out here, including the mixed ZS state approach, is described

Sect. 2. The results are presented in Sect. 3, and the concluding remarks are given in Sect. 4.

2 Method

2.1 MRI-based time-dependent anatomical model

The medical-image-based time-dependent anatomical model comes from [43]. The MRI-based method used in extracting that model can be found in [43]. The arterial cross-sectional images were acquired at 14 instants within the cardiac cycle: 0, 50, 150, 200, 250, 300, 350, 400, 450, 500, 550, 600, 725 and 850 ms, with 0 ms corresponding to the R-wave of the electrocardiogram. The time-dependent lumen geometry was constructed by associating to the points along the moving centerline cycle-averaged cross-sections. The cross-section for each point along the centerline was obtained, by averaging over the cardiac cycle, from the MRI-obtained cross-sections for that point. From that, for the computations carried out here we reconstruct the lumen geometry by mapping the cross-section for each point along the centerline to a circular cross-section. We construct the wall volume by extruding the lumen outward, with a constant wall thickness, assumed to be 0.5 mm from [42]. Then we generate a volume mesh that has 135,450 nodes and 108,000 hexahedral elements, with 4, 90 and 300 elements in the thickness, circumferential and length directions. The mesh is represented over the cardiac cycle by using cubic B-splines in time and the ST-C technique (see [46]).

2.2 Element-based ZS state estimation

An extensive description of the method for element-based ZS state estimation can be found in [28]. Here we describe some of the core concepts.

Let $\Omega_0 \in \mathbb{R}^3$ be the material domain of a structure in the ZS configuration, and let Γ_0 be its boundary. Let $\Omega_t \in \mathbb{R}^3$, $t \in (0, T)$, be the material domain of the structure in the deformed configuration, and let Γ_t be its boundary. The structural mechanics equations based on the total Lagrangian formulation can be written as

$$
\int_{\Omega_0} \mathbf{w} \cdot \rho_0 \frac{d^2 \mathbf{y}}{dt^2} \, d\Omega + \int_{\Omega_0} \delta \mathbf{E} : \mathbf{S} \, d\Omega - \int_{\Omega_0} \mathbf{w} \cdot \rho_0 \mathbf{f} \, d\Omega
$$
$$
= \int_{(\Gamma_t)_h} \mathbf{w} \cdot \mathbf{h} \, d\Gamma. \tag{1}
$$

Here, $\mathbf{y}$ is the structural displacement, $\mathbf{w}$ is the virtual displacement, $\delta \mathbf{E}$ is the variation of the Green–Lagrange strain tensor, $\mathbf{S}$ is the second Piola–Kirchhoff stress tensor, ρ_0 is the mass density in the ZS configuration, $\mathbf{f}$ is the body force

per unit mass, and $\mathbf{h}$ is the external traction vector applied on the subset $(\Gamma_t)_h$ of the total boundary Γ_t.

The deformation gradient tensor $\mathbf{F}$ is evaluated for each element:

$$\mathbf{F}^e \equiv \frac{\partial \mathbf{x}}{\partial \mathbf{X}_0^e}, \tag{2}$$

$$= \frac{\partial (\mathbf{X}_{\text{REF}} + \mathbf{y})}{\partial \mathbf{X}_0^e}, \tag{3}$$

where $\mathbf{X}_0^e$ is the ZS state for element e, and $\mathbf{X}_{\text{REF}}$ is a reference configuration. In $\mathbf{X}_{\text{REF}}$, all elements are connected by nodes, and we measure the displacement $\mathbf{y}$ from that connected configuration.

The method for element-based ZS state estimation has three parts. 1. An iterative method, which starts with an initial guess for $\mathbf{X}_0^e$, is used for computing $\mathbf{X}_0^e$ such that when the pressure load associated with $\mathbf{X}_{\text{REF}}$ is applied, $\mathbf{X}_{\text{REF}}$ is matched. During the iterations, the update method described in Section 2.2 of [28] is used. 2. A method for straight-tube geometries with single and multiple layers, described in Section 3.1 of [28], is used for computing the element-based ZS state so that we match the given diameter and longitudinal stretch in the target configuration and the opening angle. In the straight-tube computation here, we use a single layer. Two parameters are specified in computations with a single layer: the opening angle, ϕ, and the longitudinal stretch, $\lambda_z = \frac{L}{L_0}$, where L and L_0 are the tube lengths at the reference configuration and ZS state. 3. An element-based mapping between the arterial and straight-tube configurations, described in Section 3.2 of [28], is used for mapping from the arterial configuration to the straight-tube configuration, and for mapping the estimated ZS state of the straight tube back to the arterial configuration, to be used as the initial guess for the iterative method that matches $\mathbf{X}_{\text{REF}}$.

In computing the arterial dynamics, we use as $\mathbf{X}_{\text{REF}}$ the mesh at $t = 0$ s. While the calculation of $\mathbf{X}_0^e$ depends on the $\mathbf{X}_{\text{REF}}$ choice, the actual arterial dynamics computation for a given $\mathbf{X}_0^e$ does not. In the straight-tube computation we use $\phi = 270°$ and $\lambda_z = 1.2$. The value of the opening angle in our definition translates to half of that value, $\phi/2$, in the commonly-used definition, and that translation gives 135° in this case.

2.3 Material model

The arterial wall is made of Fung material. The density is 1,000 kg/m³. The Fung material constants D_1 and D_2 are 2.6447×10^3 N/m² and 8.365 (from [47]), and the penalty Poisson's ratio is 0.45.

2.4 Mixed ZS state

As mentioned in Sect. 2.2, the calculation of $\mathbf{X}_0^e$ depends on the $\mathbf{X}_{\text{REF}}$ choice. For each element e in the structural mechan-
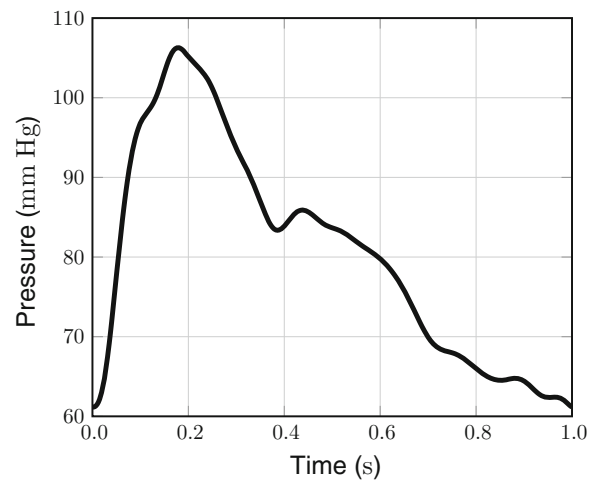

Fig. 1 Blood pressure profile

ics mesh, $\mathbf{X}_0^e$ can be estimated with a reference configuration based on the medical image coming from any instant within the cardiac cycle. We can use this freedom of choice for trying to reduce the chances of having compression regions in the arterial dynamics computation covering a cardiac cycle, which would in turn increase the robustness of the computations. This is the basic idea behind the mixed ZS state approach.

In building the mixed ZS state here, we consider four instants within the cardiac cycle where a reference configuration based on the medical image can come from: (1) 0 ms, (2) 250 ms, (3) 500 ms, and (4) 750 ms. The pressure load associated with each reference configuration is obtained from the time-dependent blood pressure profile[1] for the cardiac cycle of 1.0 s, which can be seen in Fig. 1. We calculate four different ZS sates corresponding to these four instants. Assuming that the arterial deformation during a cardiac cycle is given fully by the MRI-based time-dependent mesh deformation, for each of the four ZS states we find for every element the minimum value λ_z drops to during the cardiac cycle. For each element, we pick as the ZS state the one that gives the maximum of those four minimum-λ_z values. Figure 2 shows a view of how the elements in each of the four ZS states are distributed over the domain.

Figure 3 shows the artery after a partial longitudinal cut (LC). For more on the "LC state," see Sections 3.1 and 4.2.2 in [28]. Although we use a mixed ZS state, the opening angle

---

[1] The pressure profile is based on the subject's aortic pressure, which is known to be similar to the coronary pressure [48]. The aortic pressure was acquired using a commercial aortic pressure measurement system pulseCor (Uscom Limited, Sydney). This system calculates the aortic pressure based on the brachial pressure measured with a cuff wrapped around the subject's forearm. The system has been validated and used in clinical studies [49].
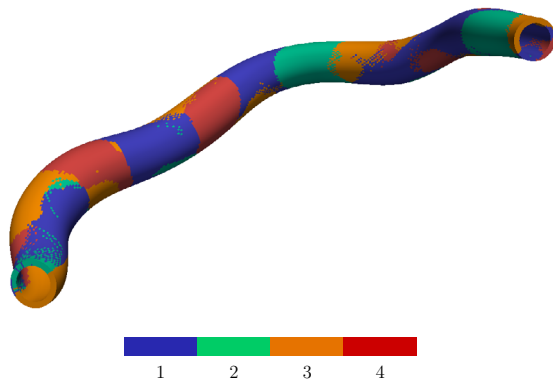
Fig. 2 A view of how the elements in each of the four ZS states are distributed over the domain. The *colors and numbers* denote the instants within the cardiac cycle where the medical-image-based reference configuration used in the ZS state estimation is coming from
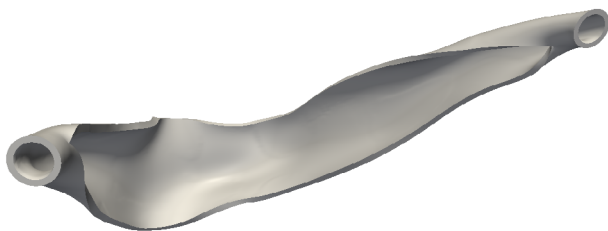
**Fig. 3** Artery after a partial longitudinal cut

is somewhat uniform, reflecting $\phi = 270°$ in calculation of all four ZS states.

2.5 Boundary conditions

On the lumen, we specify a time-dependent, uniform blood pressure; on a thin strip along the arterial surface and two cut surfaces at the arterial ends, we specify a motion that matches the motion extracted from the medical images; and elsewhere we specify zero traction. The time-dependent blood pressure profile, which was already referenced in Sect. 2.4, can be seen in Fig. 1. The parts of the boundary where we match the motion extracted from the medical images are shown in Fig. 4.

2.6 Other computational settings

In time integration of the arterial dynamics equations, we use the generalized-α method [50]. The parameters used with the method, in the notation of [22], are $\alpha_m = 2, \alpha_f = 1, \gamma = 1.5$, and $\beta = 1$. The time-step size is 2.5 ms, which translates to 400 time steps for the cardiac cycle. The number of nonlinear iterations per time step is 5, with 100, 300, 500, 500, and 500 GMRES [51] iterations in those 5 nonlinear iterations.
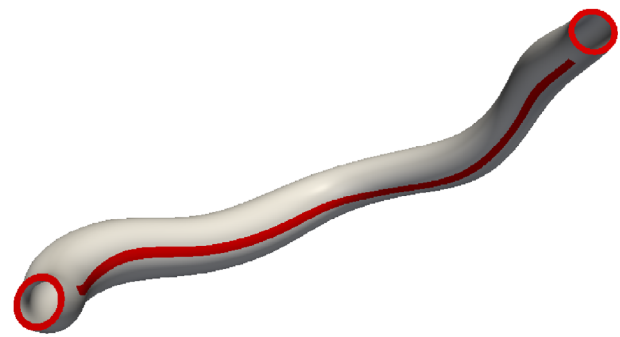
Fig. 4 The parts of the boundary where we specify a motion that matches the motion extracted from the medical images. The *strip* along the artery is 5-element wide, starts at distance of 10 elements from the *inlet* (the *left end* in the picture), and ends at a distance of 9 elements from the *outlet*

3 Results

Figure 5 shows the longitudinal stretch (λ_z). The maximum value of λ_z in space and time is approximately 1.27. The spatial average of the maximum variation of λ_z in time is about 0.04. The stretch values in some areas are not smooth because of the mixed nature of the ZS state. Those areas are essentially at the boundaries of the regions of elements in different ZS states (see Fig. 2 for the boundaries). However, the actual deformation is smooth, and is also close to the MRI-based deformation, except the radial deformation due to the time-dependent pressure. That mode of the deformation is represented in the arterial dynamics computation, but not in the MRI-based deformation. We also show, in Fig. 6, the circumferential stretch (λ_θ), even though it is less significant than the longitudinal stretch. The maximum value of λ_θ in space and time is approximately 1.34. The spatial average of the maximum variation of λ_θ in time is about 0.03.

4 Concluding remarks

Computational analysis of coronary arteries helps us gain a better understanding of the links between the atherosclerosis development and mechanical stimuli such as endothelial WSS and structural stress in the arterial wall. To increase the reliability of the analysis, we have presented a method for coronary arterial dynamics computation with time-dependent anatomical models extracted from medical images. The method has two components. The first one, introduced recently in [28], is element-based zero-stress (ZS) state estimation, which is an alternative to prestress calculation. The second one is a mixed ZS state approach, where the ZS states for different elements in the structural mechanics mesh are estimated with reference configurations based on medical images coming from different instants within the cardiac
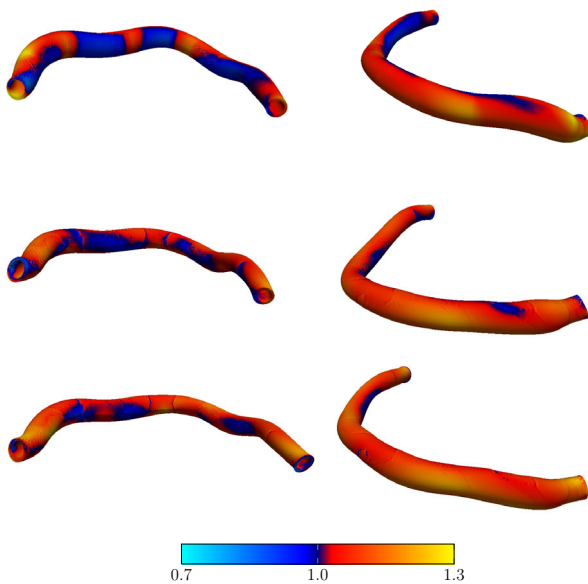
Fig. 5 *Front* (*left*) and *back* (*right*) views of the longitudinal-stretch (λ_z) patterns at $t = 0$, 375 and 750 ms
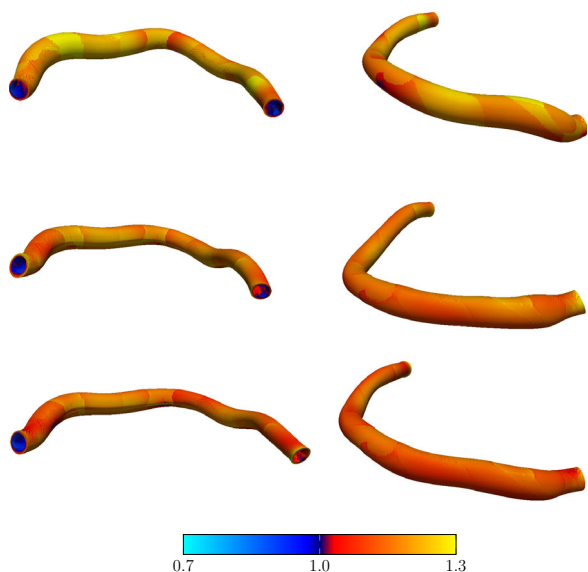
Fig. 6 *Front* (*left*) and *back* (*right*) views of the circumferential-stretch (λ_θ) patterns at $t = 0$, 375 and 750 ms

cycle. We use the freedom of choice given to us by the mixing in a process where we try to reduce the chances of having compression regions in the arterial dynamics computation covering a cardiac cycle. Reducing the chances of encountering compression increases the robustness of the computation and results in a more realistic arterial dynamics. We demonstrated the robustness of the method in a patient-specific coronary arterial dynamics computation where the motion of a thin strip along the arterial surface and two cut surfaces at the arterial ends is specified to match the motion extracted from the medical images. We expect this new ZS state esti-

mation method to become one of our frequently-used special methods targeting cardiovascular FSI modeling.

References

1. Torii R, Oshima M, Kobayashi T, Takagi K, Tezduyar TE (2006) Computer modeling of cardiovascular fluid–structure interactions with the deforming-spatial-domain/stabilized space–time formulation. Comput Methods Appl Mech Eng 195:1885–1895. doi:10.1016/j.cma.2005.05.050
2. Torii R, Oshima M, Kobayashi T, Takagi K, Tezduyar TE (2006) Fluid–structure interaction modeling of aneurysmal conditions with high and normal blood pressures. Comput Mech 38:482–490. doi:10.1007/s00466-006-0065-6
3. Bazilevs Y, Calo VM, Zhang Y, Hughes TJR (2006) Isogeometric fluid–structure interaction analysis with applications to arterial blood flow. Comput Mech 38:310–322
4. Tezduyar TE, Sathe S, Cragin T, Nanna B, Conklin BS, Pausewang J, Schwaab M (2007) Modeling of fluid–structure interactions with the space-time finite elements: arterial fluid mechanics. Int J Numer Methods Fluids 54:901–922. doi:10.1002/fld.1443
5. Bazilevs Y, Calo VM, Tezduyar TE, Hughes TJR (2007) YZβ discontinuity-capturing for advection-dominated processes with application to arterial drug delivery. Int J Numer Methods Fluids 54:593–608. doi:10.1002/fld.1484
6. Bazilevs Y, Calo VM, Hughes TJR, Zhang Y (2008) Isogeometric fluid–structure interaction: theory, algorithms, and computations. Comput Mech 43:3–37
7. Isaksen JG, Bazilevs Y, Kvamsdal T, Zhang Y, Kaspersen JH, Waterloo K, Romner B, Ingebrigtsen T (2008) Determination of wall tension in cerebral artery aneurysms by numerical simulation. Stroke 39:3172–3178
8. Bazilevs Y, Gohean JR, Hughes TJR, Moser RD, Zhang Y (2009) Patient-specific isogeometric fluid–structure interaction analysis of thoracic aortic blood flow due to implantation of the Jarvik 2000 left ventricular assist device. Comput Methods Appl Mech Eng 198:3534–3550
9. Bazilevs Y, Hsu M-C, Benson D, Sankaran S, Marsden A (2009) Computational fluid–structure interaction: methods and application to a total cavopulmonary connection. Comput Mech 45:77–89
10. Takizawa K, Christopher J, Tezduyar TE, Sathe S (2010) Space–time finite element computation of arterial fluid–structure interactions with patient-specific data. Int J Numer Methods Biomed Eng 26:101–116. doi:10.1002/cnm.1241
11. Tezduyar TE, Takizawa K, Moorman C, Wright S, Christopher J (2010) Multiscale sequentially-coupled arterial FSI technique. Comput Mech 46:17–29. doi:10.1007/s00466-009-0423-2
12. Takizawa K, Moorman C, Wright S, Christopher J, Tezduyar TE (2010) Wall shear stress calculations in space–time finite element

computation of arterial fluid–structure interactions. Comput Mech 46:31–41. doi:10.1007/s00466-009-0425-0

13. Bazilevs Y, Hsu M-C, Zhang Y, Wang W, Liang X, Kvamsdal T, Brekken R, Isaksen J (2010) A fully-coupled fluid–structure interaction simulation of cerebral aneurysms. Comput Mech 46:3–16

14. Sugiyama K, Ii S, Takeuchi S, Takagi S, Matsumoto Y (2010) Full Eulerian simulations of biconcave neo-Hookean particles in a Poiseuille flow. Comput Mech 46:147–157

15. Bazilevs Y, Hsu M-C, Zhang Y, Wang W, Kvamsdal T, Hentschel S, Isaksen J (2010) Computational fluid–structure interaction: methods and application to cerebral aneurysms. Biomech Model Mechanobiol 9:481–498

16. Bazilevs Y, del Alamo JC, Humphrey JD (2010) From imaging to prediction: emerging non-invasive methods in pediatric cardiology. Prog Pediat Cardiol 30:81–89

17. Tezduyar TE, Takizawa K, Brummer T, Chen PR (2011) Space–time fluid–structure interaction modeling of patient-specific cerebral aneurysms. Int J Numer Methods Biomed Eng 27:1665–1710. doi:10.1002/cnm.1433

18. Hsu M-C, Bazilevs Y (2011) Blood vessel tissue prestress modeling for vascular fluid–structure interaction simulations. Finite Elem Anal Des 47:593–599

19. Takizawa K, Bazilevs Y, Tezduyar TE (2012) Space-time and ALE-VMS techniques for patient-specific cardiovascular fluid–structure interaction modeling. Arch Comput Methods Eng 19:171–225. doi:10.1007/s11831-012-9071-3

20. Takizawa K, Schjodt K, Puntel A, Kostov N, Tezduyar TE (2012) Patient-specific computer modeling of blood flow in cerebral arteries with aneurysm and stent. Comput Mech 50:675–686. doi:10.1007/s00466-012-0760-4

21. Yao JY, Liu GR, Narmoneva DA, Hinton RB, Zhang Z-Q (2012) Immersed smoothed finite element method for fluid–structure interaction simulation of aortic valves. Comput Mech 50:789–804

22. Bazilevs Y, Takizawa K, Tezduyar TE (2013) Computational fluid–structure interaction: methods and applications. Wiley. ISBN:978-0470978771

23. Bazilevs Y, Takizawa K, Tezduyar TE (2013) Challenges and directions in computational fluid–structure interaction. Math Models Methods Appl Sci 23:215–221. doi:10.1142/S0218202513400010

24. Takizawa K, Schjodt K, Puntel A, Kostov N, Tezduyar TE (2013) Patient-specific computational analysis of the influence of a stent on the unsteady flow in cerebral aneurysms. Comput Mech 51:1061–1073. doi:10.1007/s00466-012-0790-y

25. Long CC, Marsden AL, Bazilevs Y (2013) Fluid–structure interaction simulation of pulsatile ventricular assist devices. Comput Mech 52:971–981. doi:10.1007/s00466-013-0858-3

26. Long CC, Esmaily-Moghadam M, Marsden AL, Bazilevs Y (2013) Computation of residence time in the simulation of pulsatile ventricular assist devices. Comput Mech. doi:10.1007/s00466-013-0931-y

27. Esmaily-Moghadam M, Bazilevs Y, Marsden AL (2013) A new preconditioning technique for implicitly coupled multidomain simulations with applications to hemodynamics. Comput Mech. doi:10.1007/s00466-013-0868-1

28. Takizawa K, Takagi H, Tezduyar TE, Torii R (2013) Estimation of element-based zero-stress state for arterial FSI computations. Comput Mech. doi:10.1007/s00466-013-0919-7

29. Takizawa K, Tezduyar TE, Buscher A, Asada S (2013) Space-time interface-tracking with topology change (ST-TC). Comput Mech. doi:10.1007/s00466-013-0935-7

30. Yao J, Liu GR (2014) A matrix-form GSM-CFD solver for incompressible fluids and its application to hemodynamics. Comput Mech. doi:10.1007/s00466-014-0990-8

31. Long CC, Marsden AL, Bazilevs Y (2014) Shape optimization of pulsatile ventricular assist devices using FSI to minimize thrombotic risk. Comput Mech. doi:10.1007/s00466-013-0967-z

32. Takizawa K, Bazilevs Y, Tezduyar TE, Long CC, Marsden AL, Schjodt K (2014) ST and ALE-VMS methods for patient-specific cardiovascular fluid mechanics modeling. Math Models Methods Appl Sci. doi:10.1142/S0218202514500250

33. Arbab-Zadeh A, Nakao M, Virmani R, Fuster V (2012) Acute coronary events. Circulation 125:1147–1156

34. Slager CJ, Wentzel JJ, Gijsen FJ, Thury A, van der Wal AC, Schaar JA, Serruys PW (2005) The role of shear stress in the destabilization of vulnerable plaques and related therapeutic implications. Nat Clin Pract Cardiovasc Med 2:1147–1156

35. Gijsen FJ, Wentzel JJ, Thury A, Mastik F, Schaar JA, Shuurbiers JC, Slager CJ, van der Giessen WJ, de Feyter PJ, van der Steen AF, Serruys PW (2008) Strain distribution over plaques in human coronary arteries relates to shear stress. Am J Physiol Heart Circ Physiol 295:H1608–H1614

36. VanEpps JS, Londono R, Nieponice A, Vorp DA (2009) Design and validation of a system to simulate coronary flexure dynamics on arterial segments perfused ex vivo. Biomech Model Mechanobiol 8:57–66

37. Yang C, Bach RG, Zheng J, Naqa IE, Woodard PK, Teng Z, Billiar K, Tang D (2009) In vivo ivus-based 3-d fluid–structure interaction models with cyclic bending and anisotropic vessel properties for human atherosclerotic coronary plaque mechanical analysis. IEEE Trans Biomed Eng 56:2420–2428

38. Torii R, Wood NB, Hadjiloizou N, Dowsey AW, Wright AR, Hughes AD, Davies J, Francis DP, Mayet J, Yang GZ, Thom SAM, Xu XY (2009) Fluid–structure interaction analysis of a patient-specific right coronary artery with physiological velocity and pressure waveforms. Commun Numer Methods Eng 25:565–580

39. Krams R, Wentzel JJ, Oomen JA, Vinke R, Schuurbiers JC, de Feyter PJ, Serruys PW, Slager CJ (1997) Evaluation of endothelial shear stress and 3d geometry as factors determining the development of atherosclerosis and remodeling in human coronary arteries in vivo. combining 3d reconstruction from angiography and ivus (angus) with computational fluid dynamics. Arterioscler Thromb Vasc Biol 17:2061–2065

40. Torii R, Wood NB, Hadjiloizou N, Dowsey AW, Wright AR, Hughes AD, Davies J, Francis D, Mayet J, Yang GZ, Thom SA, Xu XY (2009) Stress phase-angle depicts differences in coronary artery hemodynamics due to changes in flow and geometry after percutaneous coronary intervention. Am J Physiol Heart Circ Physiol 296:H765–H776

41. Zeng D, Ding Z, Friedman MH, Ethier CR (2003) Effects of cardiac motion on right coronary artery hemodynamics. Ann Biomed Eng 31:420–429

42. Zhu H, Friedman MH (2003) Relationship between the dynamic geometry and wall thickness of a human coronary artery. Arterioscler Thromb Vasc Biol 23:2260–2265

43. Torii R, Keegan J, Wood NB, Dowsey AW, Hughes AD, Yang G-Z, Firmin DN, Thom SAM, Xu XY (2010) MR image-based geometric and hemodynamic investigtion of the right coronary artery with dynamic vessel motion. Ann Biomed Eng 38:2606–2620

44. Tezduyar TE, Sathe S, Schwaab M, Conklin BS (2008) Arterial fluid mechanics modeling with the stabilized space–time fluid–structure interaction technique. Int J Numer Methods Fluids 57:601–629. doi:10.1002/fld.1633

45. Takizawa K, Moorman C, Wright S, Purdue J, McPhail T, Chen PR, Warren J, Tezduyar TE (2011) Patient-specific arterial fluid–structure interaction modeling of cerebral aneurysms. Int J Numer Methods Fluids 65:308–323. doi:10.1002/fld.2360

46. Takizawa K, Tezduyar TE (2014) Space–time computation techniques with continuous representation in time (ST-C). Comput Mech 53:91–99. doi:10.1007/s00466-013-0895-y

47. Huang H, Virmani R, Younis H, Burke AP, Kamm RD, Lee RT (2001) The impact of calcification on the biomechanical stability of atherosclerotic plaques. Circulation 103:1051–1056

48. Davies JE, Whinnett ZI, Francis DP, Manisty CH, Aguado-Sierra J, Willson K, Foale RA, Malik IS, Hughes AD, Parker KH, Mayet J (2006) Evidence of a dominant backward-propagating "suction" wave responsible for diastolic coronary filling in humans, attenuated in left ventricular hypertrophy. Circulation 113:1768–1778

49. Roman MJ, Devereux RB, Kizer JR, Okin PM, Lee ET, Wang W, Umans JG, Calhoun D, Howard BV (2009) High central pulse pressure is independently associated with adverse cardiovascular outcome the strong heart study. J Am Coll Cardiol 54:1730–1734

50. Chung J, Hulbert GM (1993) A time integration algorithm for structural dynamics with improved numerical dissipation: the generalized-α method. J Appl Mech 60:371–375

51. Saad Y, Schultz M (1986) GMRES: a generalized minimal residual algorithm for solving nonsymmetric linear systems. SIAM J Sci Stat Comput 7:856–869